available at www.sciencedirect.com

ScienceDirect

journal homepage: www.elsevier.com/locate/biochempharm

Curcumin-induced degradation of PKCδ is associated with enhanced dentate NCAM PSA expression and spatial learning in adult and aged Wistar rats

Lisa Conboy, Andrew G. Foley, Noel M. O'Boyle, Marie Lawlor, Helen C. Gallagher, Keith J. Murphy, Ciaran M. Regan *

School of Biomolecular and Biomedical Sciences, UCD Conway Institute, University College Dublin, Belfield, Dublin 4, Ireland

ARTICLE INFO

Article history:
Received 7 November 2008
Accepted 19 December 2008

Keywords:
PKCδ
PST
NCAM PSA
Curcumin
Spatial learning

ABSTRACT

Polysialylation of the neural cell adhesion molecule (NCAM PSA) is necessary for the consolidation processes of hippocampus-based learning. Previously, we have found inhibition of protein kinase C delta (PKCδ) to be associated with increased polysialyltransferase (PST) activity, suggesting inhibitors of this kinase might ameliorate cognitive deficits. Using a rottlerin template, a drug previously considered an inhibitor of PKCδ, we searched the Compounds Available for Purchase (CAP) database with the Accelrys® Catalyst programme for structurally similar molecules and, using the available crystal structure of the phorbol-binding domain of PKCδ, found that diferuloylmethane (curcumin) docked effectively into the phorbol site. Curcumin increased NCAM PSA expression in cultured neuro-2A neuroblastoma cells and this was inversely related to PKCδ protein expression. Curcumin did not directly inhibit PKCδ activity but formed a tight complex with the enzyme. With increasing doses of curcumin, the Tyr^{131} residue of PKCδ, which is known to direct its degradation, became progressively phosphorylated and this was associated with numerous Tyr^{131}-phospho-PKCδ fragments. Chronic administration of curcumin *in vivo* also increased the frequency of polysialylated cells in the dentate infragranular zone and significantly improved the acquisition and consolidation of a water maze spatial learning paradigm in both adult and aged cohorts of Wistar rats. These results further confirm the role of PKCδ in regulating PST and NCAM PSA expression and provide evidence that drug modulation of this system enhances the process of memory consolidation.

1. Introduction

A significant post-translational modification of the neural cell adhesion molecule (NCAM) involves the attachment of large homopolymers of α2,8-linked polysialic acid (PSA), a modification that is specific to NCAM in the mammalian brain [1,2]. This post-translational modification of NCAM has been extensively argued to support structural plasticity in the adult nervous system [3–5] and has been implicated in activity-dependent synaptic remodelling [6,7]. Moreover, the synaptic remodelling that accompanies task consolidation of spatial learning and avoidance conditioning paradigms [8–10] is

* *Corresponding author*. Tel.: +353 1 7166775; fax: +353 1 7166920.
E-mail address: ciaran.regan@ucd.ie (C.M. Regan).

Abbreviations: DMEM, Dulbecco's modified Eagle's medium; NCAM, neural cell adhesion molecule; PKC, protein kinase C; PSA, poly-α2,8-linked sialic acid; PST, polysialyltransferase; curcumin, ([diferuloylmethane] 1,7-bis-[4-hydroxy-3-methoxyphenyl]-1,6-heptadiene-3,5-dione); rottlerin, ([mallotoxin] 5,7-dihydroxy-2,2-dimethyl-6-[2,4,6-trihydroxy-3-methyl-5-acetylbenzyl]-8-cinnamoyl-1,2-chromine).

0006-2952/$ – see front matter
doi:10.1016/j.bcp.2008.12.011

associated with a transient increase in the frequency of dentate granule cells expressing polysialylated NCAM at the 12 h post-training time [11–13] and cleavage of PSA with endoneuraminidase-N impairs the development of long-term potentiation (LTP), a cellular analogue of memory and learning, and the consolidation of spatial learning and avoidance conditioning paradigms [14–17]. Intraventricular infusion of anti-PSA, when administered specifically at the 10 h post-training time, has also been demonstrated to impair the consolidation of spatial and avoidance conditioning tasks, further confirming the time-dependent functional requirement of NCAM PSA in memory formation [18]. Polysialylation of NCAM occurs in the trans-Golgi compartment and is catalysed by two enzymes termed sialyltransferase-X (STX or ST8SiaII) [19,20] and polysialyltransferase (PST or ST8SiaIV) [21,22]. These two PSTs regulate NCAM polysialylation state differentially during development, as STX is the dominant PST in the embryonic and early postnatal period, whereas PST is mainly associated with α2,8-polysialylation in the postnatal brain [23,24]. Pulse-labelling studies *in vitro* have indicated PSA synthesis to occur in the late-Golgi, or post-Golgi, compartment where NCAM becomes rapidly glycosylated with the newly synthesized PSA [25].

In general, the molecular events associated with regulation of sialyltransferase-mediated glycosylation still remain to be fully elucidated. The proposed involvement of PKC in the regulation of PST-mediated NCAM polysialylation state stems from the observation that phorbol-12-myristate-13-acetate, which activates diacylglycerol-dependent PKC isoforms, induces a dose-dependent decrease in NCAM PSA expression in neuro-2A neuroblastoma cells and staurosporine, a pan-specific PKC inhibitor, increases NCAM polysialylation state [26] Moreover, immunoblotting procedures have demonstrated reduced PKCδ expression to be associated with the enhanced polysialylation of NCAM *in vitro* and, using a polyclonal antibody directed against a conserved 11-amino acid sequence in *Escherichia coli* PST, hippocampal PKCδ has been found to form complexes with PST that increase as animals age [27] and NCAM PSA expression decreases in an exponential manner [28]. The PST associated with these complexes has also been observed to be phosphorylated on serine residues [27], a mechanism known to be associated with the inhibition of other sialyltransferases [29–32]. Phosphorylated tyrosine residues on PST are also found in PST:PKCδ immunocomplexes [27] and this may play a crucial role in regulating PKCδ expression as phosphorylation of conserved tyrosine residues in the hinged bilobal structure, typical of the PKC family of isozymes, confers a specific post-translational control on the rate of proteolytic cleavage [33,34].

In previous studies directed to providing evidence for a role of PKCδ in the regulation of NCAM polysialylation in neuro-2A neuroblastoma cells [26], we employed rottlerin to inhibit PKCδ, as this had been reported to have an IC_{50} value of 3–6 μM and to be 5–17 times more potent as a PKCδ inhibitor over other PKC isozymes [35]. Neuro-2A cells exposed to rottlerin (5 μM) in the mid-log growth phase, when NCAM PSA expression is dominant, resulted in a rapid and substantial increase in NCAM polysialylation state [26]. Moreover, exposure of the same concentration of rottlerin to cells in contact inhibition, where no NCAM PSA is expressed, resulted in PST activation and expression of polysialylated NCAM. Subsequent studies, however, have failed to confirm rottlerin to be a direct inhibitor of PKCδ [36] but that it may modulate the tyrosine phosphorylation state of PKCδ and indirectly affect enzyme activity [37]. We now demonstrate curcumin to be a chemical similar of rottlerin that indirectly modulates PKCδ activity by modifying its phosphorylation state to increase the rate of degradation.

2. Materials and methods

2.1. Materials

All routine laboratory chemicals, secondary antibodies, rottlerin, staurosporine and curcumin were purchased from Sigma–Aldrich, Ireland. All components of the PKCδ activity assay, including constitutively active recombinant PKCδ, were purchased from Upstate Biotechnology (Charlottesville, VA, USA). [γ-^{32}P]-ATP was purchased from Amersham Biosciences (Buckinghamshire, UK). The bicinchoninic acid (BCA) assay was purchased from Pierce (Rockford, IL, USA). The monoclonal antibody raised against the meningococcus group B polysaccharides (anti-PSA) was a kind gift from Prof. G. Rougon [2]. Monoclonal primary antibody to PKCδ was purchased from BD Biosciences (Oxford, UK).

2.2. In silico studies

2.2.1. Database searching with catalyst and protein–ligand docking with Cerius2

Computational studies were carried out using a Silicon Graphics Octane workstation (SGI, Mountain View, CA, USA). Catalyst version 3.4 (Accelrys®, Cambridge, UK) was used to search the Compounds Available for Purchase (CAP) database to identify those structurally similar to rottlerin using a template structure based on its side chain (see Fig. 1A). Prior to database screening, the search was restricted to drug-like molecules based on the Lipinski rules [38]. Using Cerius2 (version 4.8; Accelrys®, UK), the matching compounds were rated using protein–ligand docking to the crystal structure of the PKCδ ligand-binding domain, which was downloaded from the Brookhaven Protein Data Bank. In preparation for docking, all organic and inorganic cofactors, the phorbol ester ligand, as well as all water molecules, were removed from the PKCδ crystal structure. Potential PKCδ inhibitors were sequentially docked to the PKCδ crystal structure and ligand–enzyme interactions were quantified using the DOCK scoring function of the LigFit module of Cerius2. The top ranking compounds were screened in *in vitro* assays, described below, to determine their potential to modulate NCAM PSA.

2.3. In vitro analysis of NCAM PSA expression

The mouse neuroblastoma cell line, neuro-2A, was maintained in Dulbecco's modified Eagle's medium (DMEM; Gibco, UK) supplemented with 10% (v/v) foetal calf serum (Gibco, UK) and penicillin/streptomycin (100 mg/ml; Sigma, UK) at 37 °C in a humidified atmosphere and 9% CO_2. To investigate pharmacological modulation of PSA expression, cells were seeded on 96-well plates at a density of 10^4 cells/cm^2 and grown until

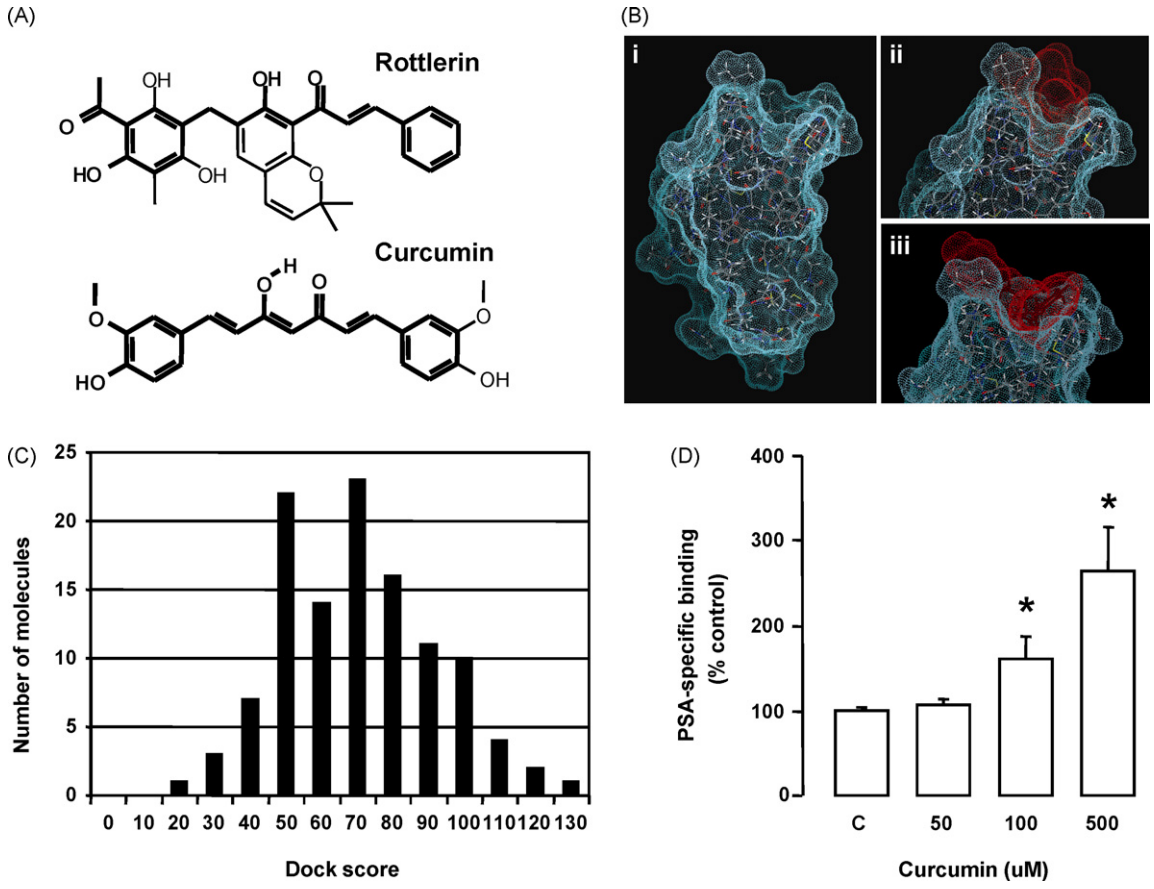

Fig. 1 – *In silico* approach to identification of curcumin as a rottlerin analogue. The chemical structure of rottlerin and curcumin with the pharmacopore side chain in bold is shown in (A). Crystal structure of the PKCδ CIB binding site is shown in(Bi) along with its interaction with the phorbol ester (Bii) and curcumin (Biii). (C) A histogram plot of the 137 rottlerin-like molecules and their strength of their interaction, based on dock score, with the PKCδ C1B domain (C). (D) The curcumin-induced, dose-dependent increase in PSA expression in neuro-2A neuroblastoma cells.

day 3 *in vitro* (DIV 3). On DIV3, cells were treated with either vehicle (DMSO not exceeding 1% v/v) or test PKCδ inhibitor ranging in dose from 1 to 500 μM for 5 h. Specifically, curcumin was administered at concentrations of 1, 10, 50, 100 and 500 μM. Cells were then fixed with 200 μl of 4% paraformaldehyde in DMEM for 60 min at room temperature. This was replaced with undiluted fixative for a further 60 min. Non-specific binding sites were blocked with 2% (w/v) bovine serum albumin (Sigma–Aldrich, Ireland) and 2% (v/v) normal goat serum (Sigma–Aldrich, Ireland) in phosphate buffered saline (PBS) (blocking solution, in which all antibodies were also diluted). PSA was detected using a monoclonal antibody raised against the meningococcus group B polysaccharides (anti-PSA) prepared as an ascitic fluid and diluted 1:500. Primary antibody was incubated overnight at 4 °C. Binding of the primary antibody was detected using a secondary goat anti-mouse immunoglobulin G (IgG) conjugated to peroxidase diluted 1:2000 for 1 h at room temperature. Peroxidase activity was determined using the liquid substrate tetramethylbenzidine (Sigma–Aldrich, Ireland), which was incubated for 30 min at room temperature and the reaction was terminated by acidification with 2 M H_2SO_4. Optical density was measured in a microplate reader with a 450 nm measurement filter and 620 nm reference filter.

2.4. PKCδ activity assay

Constitutively active recombinant PKCδ was derived from Sf21 cells and assay of enzyme activity was performed according to the manufacture's instructions. In brief, 0–20 ng of recombinant PKCδ was incubated with 50 μM PKC substrate peptide (myelin basic protein), in the presence of 200 μM ATP, 30 mM magnesium chloride, 0.05 mg/ml phosphatidylserine, 0.005 mg/ml diacylglycerol and [γ-^{32}P]-ATP (Amersham Biosciences, UK) for 10 min at 30 °C. Following incubation, 20 μl of each assay was spotted onto phosphocellulose paper and the reaction terminated by washing of the phosphocellulose in 0.75% phosphoric acid for 5 min. Following two subsequent 5 min washes in phosphoric acid, the samples were washed in acetone for a further 5 min. The phosphocellulose paper was dried, transferred to scintillation fluid and the radioactivity counted. Under these conditions, increasing concentrations of PKCδ were associated with increasing levels of radioactivity. Using 20 ng of recombinant PKCδ and the conditions described above, staurosporine (5 nM), rottlerin (10 and 100 μM) and curcumin (10 and 500 μM) were included in the assay and their ability to inhibit PKCδ kinase activity in a dose-dependent manner was determined. In additional experiments, the assay

concentration of ATP was lowered to 40 μM ATP to determine potential competition at the ATP binding site.

2.5. Immobilisation of curcumin on epoxy-activated Sepharose™ 6B

To investigate curcumin–PKCδ interactions, curcumin was coupled to epoxy-activated Sepharose™ 6B (Sigma–Aldrich, Ireland). Using a previously described method [39], a 1 g aliquot of epoxy-activated Sepharose™ 6B beads was washed in 50 ml of dH_2O for five cycles to give approximately 3.5 ml of swollen beads. For coupling to the epoxy-activated beads, curcumin was prepared as a 20 mM solution in 50% dimethylformamide/0.1 M Na_2CO_3/10 mM NaOH and two volumes of this solution was mixed with one volume of swollen beads and incubated overnight at 30 °C in the dark. The following day, the curcumin–Sepharose suspension was washed three times with coupling buffer and the remaining non-specific binding sites were blocked by incubation with 1 M ethanolamine overnight at 30 °C. Control beads were prepared by incubating the epoxy-activated Sepharose™ 6B with 1 M ethanolamine, pH 11. The control and curcumin-coupled beads were finally washed in three cycles of alternating low (0.1 M acetate buffer, pH 4.0) and high (0.1 M Tris–HCl buffer, pH 8, containing 0.5 M NaCl) pH buffers. Hippocampal PKCδ was prepared by homogenising rat dentate gyrus in 100 mM Hepes buffer, pH 7.6, containing 300 mM NaCl, 1% Triton-X-100, 2 mM EDTA, 2 mM EGTA and 0.1 mM PMSF, 50 mM Na_3VO_4 and 1 μg/μl aprotinin as protease inhibitors (2× lysis buffer). A 250 μl aliquot of cell lysate was incubated with 20 μl of curcumin-coupled Sepharose, or control beads, with constant mixing for 3 h at 4 °C. Afterwards, the curcumin–Sepharose complex was washed twice with 500 μl of 2× lysis buffer (without protease inhibitor) containing 150 mM NaCl (low salt) followed by 500 μl of 1× lysis buffer containing 1 M NaCl (high salt). Proteins were isolated from the bead–protein complex by resuspending and boiling the washed beads in SDS-PAGE sample buffer. PKCδ was detected by the immunoblotting procedure described below.

2.6. Immunoblot analysis of PKCδ expression

Neuro-2A cells were seeded in 75 cm^2 plates (10^4 cells/cm^2) and exposed to increasing concentrations of curcumin for 5 h during the mid-log growth phase, as described above. The cells were then washed three times in PBS, scraped and pelleted by centrifugation for 10 min at 900 rpm. The pellet was solubilised in RIPA buffer (50 mM Tris, pH 8.0, containing 50 mM NaCl, 1.0% NP-40, 0.5% sodium deoxycholate and 0.1% SDS), containing protease inhibitors for 30 min on ice. The supernatant was then collected by centrifugation at 3000 × *g* and the protein concentrations determined by the BCA assay. Samples, of equal protein concentration, were boiled for 10 min in a reducing sample buffer of 70 mM Tris–HCl, pH 6.8, containing 33 mM NaCl, 1 mM EDTA, 2% (w/v) SDS, 0.01% (w/v) bromophenol blue, 10% glycerol and 3% (v/v) dithiothreitol reducing agent (New England Biolabs, UK). Samples containing equal amounts of protein were separated on 10% polyacrylamide minigels and electrophoretically transferred to nitrocellulose membranes and successful transfer was confirmed by ponceau S staining of the membrane (not shown). The nitrocellulose was then blocked using washing buffer [10 mM Tris–HCl, pH 7.4, containing 150 mM NaCl, and 0.05% (v/v) Tween-20] with 5% (w/v) non-fat milk powder for 1 h at room temperature. The monoclonal primary antibody to PKCδ was diluted 1:1000 in blocking buffer and incubated overnight at 4 °C with the nitrocellulose membrane. The primary antibody was then detected using goat anti-mouse IgG peroxidase-conjugated secondary antibody. Following membrane washing, the immunocomplexes were detected using a chemiluminescence peroxidase substrate and exposure of the membranes to X-ray film (Kodak, Dublin, Ireland). Equal protein loading was verified by stripping the blots and re-probing them with an anti-actin monoclonal antibody (Sigma–Aldrich, Ireland) diluted 1: 20,000. The developed X-ray films were scanned using Adobe Photoshop 7.0.

2.7. Quantitative immunohistochemical analysis of NCAM PSA in vivo

Male Wistar rats (postnatal day 80) were obtained from the Biomedical Facility, University College Dublin, and housed singly in a 12 h light/dark cycle at 22 ± 2 °C, with *ad libitum* access to food and water. Curcumin (75 mg/kg), dissolved in a methylcellulose (0.5% w/v) vehicle, was administered daily by gavage for an 8-day period. Control animals received the methylcellulose vehicle for the same 8-day period. At 24 h after the final drug administration, the animals were sacrificed by cervical dislocation and the whole brain was quickly dissected. The brains were coated immediately in an optimal cutting temperature compound (Gurr, Poole, UK), snap-frozen in CO_2-cooled *n*-hexane, and stored at −80 °C until required for further processing. The frequency of hippocampal polysialylated neurons was determined using PSA immunohistochemistry, as described previously [11]. Briefly, cryostat axial sections of 12 μm were fixed in 70% (v/v) ethanol and incubated overnight with anti-PSA ascitic fluid diluted 1:500 in PBS. The sections were exposed for 3 h to fluorescein-conjugated goat anti-mouse IgM diluted 1:100 in PBS and mounted in Citifluor® (Citifluor Ltd., UK), a fluorescence-enhancing medium. The total numbers of PSA-immunopositive neurons at the infragranular cell layer of the dentate gyrus, at −5.6 mm with respect to bregma, were counted in seven alternate 12 μm sections. The sections were counter stained with propidium iodide (60 s, 40 ng/ml) (Sigma–Aldrich, Ireland) to facilitate cell identification and the use of alternate sections precluded double counting of the 5–10 μm perikarya. Cell counts were expressed per unit area of the dentate granule cell layer (0.15 mm^2) and the mean ± SEM for each treatment group calculated.

2.8. Water maze spatial learning paradigm

Separate cohorts of male Wistar rats (postnatal days 80 and 540), sourced and maintained as described above, were used in these studies. On each of the 2 days preceding commencement of water maze studies, animals were handled and assessed in an open field arena for locomotor activity, rearing and general behaviour over a 5 min period. Each cohort of animals was treated for 8 days with 75 mg/kg curcumin by gavage. An extended 40-day treatment period did not confer

any additional advantage on the parameters under investigation (data not shown). The control groups received vehicle alone. Water maze training was initiated at 24 h following the final drug administration. The water maze apparatus consisted of a large circular pool (1 m diameter, 80 cm high, water temperature 26 ± 1 °C) with a platform (11 cm diameter) submerged 1.5 cm below the water surface [12]. The water was 50 cm deep and the wall of the pool was 30 cm above the level of the water. Both the pool and the platform were constructed of black polyvinyl plastic and offered no intra-maze cues to guide escape behaviour. The experimental room contained several extra-maze visual cues. During testing, the platform was hidden in the same quadrant 30 cm from the sidewall. Animals were trained in four training sessions separated by 24 h and each session, consisting of five trials, was separated by an inter-trial test interval of 300 s. Each trial started with the rat facing the wall of the maze at one of three fixed points A, B or C arranged triangularly around the pool (separated by 120°). The starting positions were used sequentially over the five trials of each training session and continuity in the pattern of starting positions was maintained over different sessions so that all starting points were used the same number of times. Computerised tracking software (Watermaze 3.1) was used to measure relevant parameters that included swim angle, swim speed, escape latency and path length. The time taken by the rat to find the hidden platform within a 60 s criterion period was defined as the escape latency time. On the first trial, rats failing to locate the platform within the 60 s period were placed on it for 10 s. Escape latencies were measured over five trials in each training session. Probe trials were performed at 1 and 3 days following the final training session. In these trials, the platform was removed and the time spent in each quadrant of the pool was tracked over a 60 s period.

All experimental procedures were approved by the Animal Research Ethics Committee of University College Dublin and were carried out by individuals holding the appropriate national license issued by the Department of Health.

2.9. Statistics

All statistical analysis was carried out using GraphPad Prism (version 4) software. Curcumin effects on NCAM PSA and PKCδ expression were analysed by using Student's unpaired two-tailed *t*-test. Kinase activity assay values were analysed by ANOVA followed by Dunnett's post-hoc analysis. The effect of drug treatment and trial number on escape latency from the water maze was assessed by repeated measures ANOVA. Specific trials and probe differences were analysed using Student's unpaired two-tailed *t*-test. In all cases, *P* values less than 0.05 were considered to be significant.

3. Results

3.1. Identification of curcumin as a chemical similar of rottlerin

Taking rottlerin as our template structure, we used the substructure highlighted in bold in Fig. 1A to search the CAP database for structurally similar chemicals using the Accelrys® Catalyst programme. This allowed the identification of 137 compounds. This list of compounds was further refined using the Accelrys® Cerius2 modelling and simulation programme to test for ligand fit to the crystallised C1B phorbol-binding domain of the PKCδ molecule (Fig. 1Bi). The C1B domain of the regulatory region of PKCδ, containing the phorbol ester, was obtained from the Protein Data Base (PKCδ C1B domain RCSB PDB entry 1PTQ, [40], Fig. 1Bii). The phorbol ester was removed and the binding site defined using the site search function of Cerius2. The energy of the PKCδ crystal structure was minimised using the Dreiding 2.21 force field and energy minimised rottlerin conformers were docked to the PKCδ phorbol-binding site. The ligand–enzyme score was quantified using the 'DOCK' score of the Cerius2 LigFit module, which rated interaction energy and internal ligand energy between enzyme and ligand. DOCK scores of the 137 identified compounds with the PKCδ C1B phorbol-binding domain showed a normal distribution (Fig. 1C). Within this distribution, both curcumin and rottlerin exhibited high DOCK scores of 92 and 87, respectively, indicating significant chemical similarity between these compounds. The interaction of curcumin with the PKCδ C1B phorbol-binding domain is illustrated in Fig. 1Biii. Using an ELISA-based assay, curcumin was also found to enhance NCAM PSA expression in a dose-dependent manner in neuro-2A neuroblastoma cells (Fig. 1D). This confirmed curcumin to have the same biological activity of rottlerin, as reported previously [26], and that both compounds most likely influenced PKCδ activity in a similar manner. The dose of curcumin required to enhance NCAM PSA expression was, however, an order of magnitude greater than that previously reported for rottlerin (5 μM, [26]). This difference in dose–response is most likely related to the unstable nature of curcumin at neutral and basic pH both of which lead to its rapid degradation and formation of ferulic acid, a potent antioxidant [41]. Ferulic acid, however, failed to enhance NCAM PSA expression in the neuro-2A neuroblastoma cell line (data not shown) further confirming the primary role of curcumin in this effect.

3.2. Influence of curcumin and rottlerin on PKCδ kinase activity

Given that previous studies demonstrated rottlerin to be without effect on PKCδ activity [36,37], we determined if curcumin similarly failed to influence enzyme activity. The *in vitro* assay employed determined the influence of curcumin on the phosphorylation rate of myelin basic protein using purified human recombinant PKCδ protein (Fig. 2A) in the presence of [γ-^{32}P]-ATP and phosphatidylserine and diacylglycerol (DAG) lipid activators. Using this assay, the phosphorylation rate of myelin basic protein substrate was found to be directly related to the concentration of PKCδ enzyme present (Fig. 2B). We further validated the assay using the non-specific PKC inhibitor staurosporine and found it to inhibit PKCδ kinase activity in a dose-dependent manner (data not shown). Staurosporine exhibited an IC_{50} value of approximately 5 nM, which is in close agreement with the IC_{50} value of 3.5 nM reported previously [42]. At 5 nM, staurosporine reduced PKCδ kinase activity to $47.3 \pm 9.2\%$ of that observed in the control sample (Fig. 2C). In comparison to rottlerin and curcumin, over

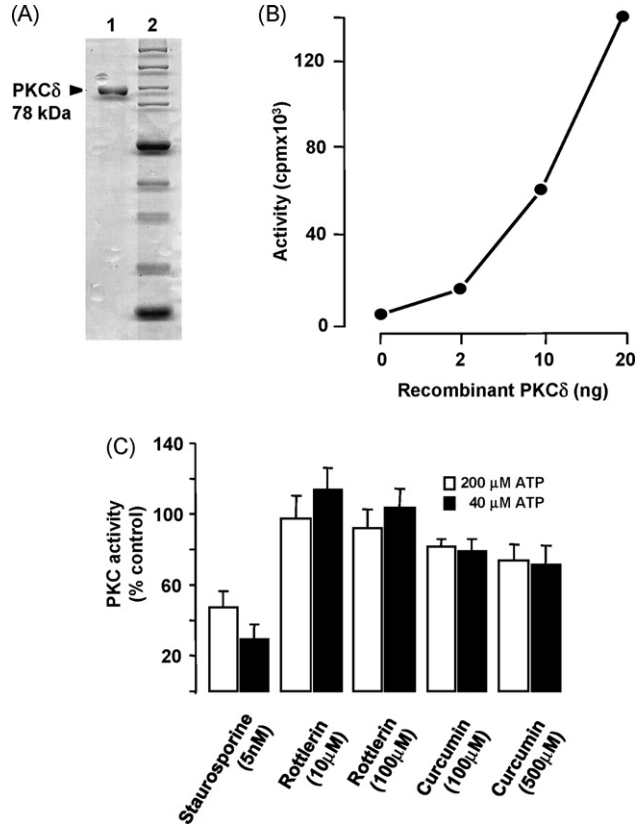

Fig. 2 – Influence of curcumin and rottlerin on recombinant PKCδ activity. (A) The purity of the enzyme preparation (lane 1, enzyme preparation; lane 2, molecular weight markers) and (B) enzyme activity with increasing concentrations of recombinant PKCδ. (C) Inhibition of enzyme activity, in the presence of 40 μM (filled columns) and 200 μM (open columns) ATP, using staurosporine as a positive control; (C) also shows rottlerin and curcumin to be without effect on PKCδ activity. The data are expressed as the mean ± SEM ($n = 3$) and values significantly different ($P < 0.05$) from the vehicle-treated controls are indicated with an asterisk.

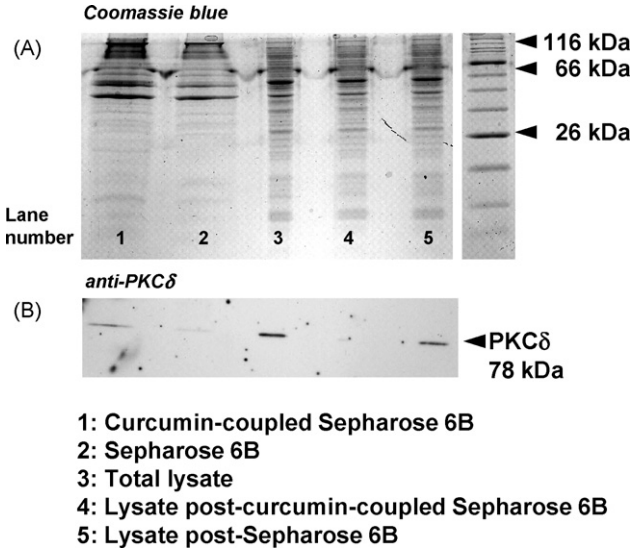

Fig. 3 – Association of curcumin-conjugated Sepharose™ 6B with PKCδ in lysates from the hippocampal dentate gyrus. (A) The Coomassie blue-stained gel analysis of bead-associated protein (lanes 1 and 2) and the remaining lysate following bead incubation (lanes 4 and 5). Lane 3 shows the protein profile of the lysate. All lanes had equal protein loading. (B) The immunoblot analysis of the same lanes with anti-PKCδ.

concentration ranges of 10–100 or 100–500 μM, respectively, only staurosporine inhibited PKCδ activity ($F[5,12] = 11.09$, $P < 0.05$). To further preclude the possibility that rottlerin or curcumin may be acting as competitive inhibitors at the PKCδ ATP binding site, we determined the consequence of lowering available ATP (200 to 40 μM) on kinase activity. At this lower ATP concentration, staurosporine further reduced PKCδ kinase activity to 29.5 ± 8.4% of the control value but it was without effect on the ability of curcumin or rottlerin to inhibit PKCδ activity (Fig. 2C). These results demonstrated rottlerin to be without any direct effect on PKCδ activity, confirming previous reports [36], and that the related compound curcumin similarly failed to influence enzyme activity.

3.3. *Curcumin binding promotes PKCδ degradation*

Given curcumin failed to inhibit PKCδ activity, despite its high DOCK score for the phorbol-binding site of the enzyme, we determined if curcumin formed a complex with the enzyme. To achieve this, we covalently coupled curcumin to epoxy-activated Sepharose™ 6B, via its available hydroxyl groups, and used these beads to bait PKCδ in lysates of rat dentate gyrus solubilised with a non-ionic detergent, a procedure employed previously to identify the cellular targets of other protein kinase inhibitors [39]. Incubation of the dentate lysate with curcumin-coupled Sepharose resulted in PKCδ forming a tight linkage to curcumin. Following removal of weakly bound proteins by a cycle of low- and high-salt wash and rigorous boiling in SDS gel sample buffer, the remaining Coomassie blue-stained electrophoretic protein profile was found to be comparable across all treatment conditions (Fig. 3A, equal protein loading). Immunoblot analysis with anti-PKCδ, however, revealed the enzyme to be associated with the curcumin-coupled Sepharose™ 6B and not with the control Sepharose™ 6B (Fig. 3B, lanes 1 and 2). Moreover, the curcumin-coupled Sepharose™ 6B bound all of the PKCδ in the lysate as immunoblot analysis of the remainder failed to detect any enzyme immunoreactivity (Fig. 3B, lane 4) and this was in contrast to the abundant PKCδ immunoreactivity observed in the lysate following incubation with the control Sepharose™ 6B (Fig. 3B, lane 5). Moreover, the tight association of PKCδ with curcumin appeared to exert an allosteric effect that rendered the enzyme more amenable to Tyr^{311} phosphorylation. Exposure of the neuro-2A neuroblastoma cell line to curcumin for a 5 h period resulted in a dose-dependent decrease in PKCδ protein expression with no effect being observed on actin protein levels (Fig. 4A and B). This increase in PKCδ protein degradation was paralleled by a dose-dependent increase in

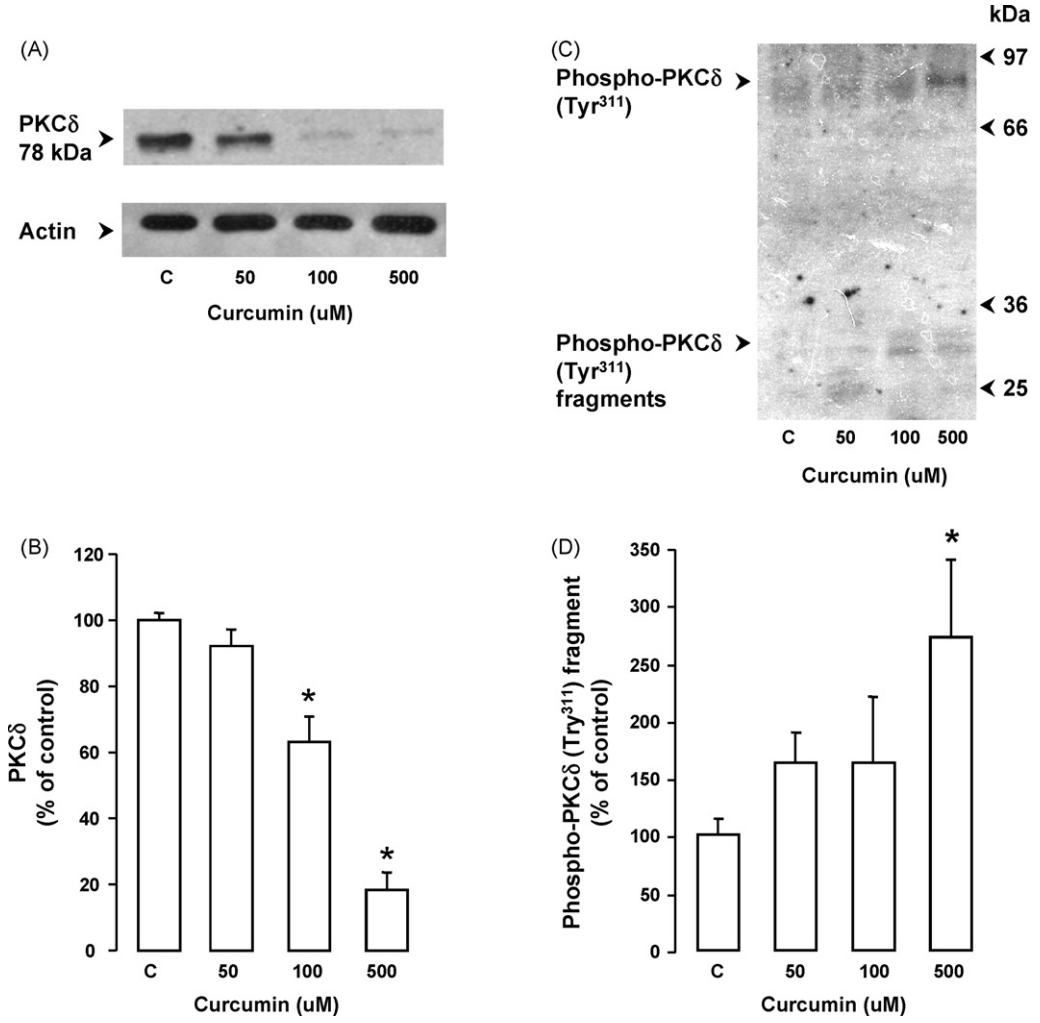

Fig. 4 – Influence of curcumin on PKCδ expression in neuro-2A neuroblastoma cells. The immunoblot in (A) illustrates a curcumin-induced, dose-dependent decrease in PKCδ enzyme protein and the histogram in (B) shows the same data expressed in a semi-quantitative densitometric manner. Equal protein loading is shown with the actin immunoblot in (A). (C) The dose-dependent increase in PKCδ tyrosine^{311} phosphorylated PKCδ and its fragments in the presence of curcumin and (D) is a semi-quantitative densitometric of the same data. All data are expressed as the mean ± SEM ($n = 3$) and values significantly different ($P < 0.05$) from the vehicle-treated controls are indicated with an asterisk.

the phosphorylation of the Tyr^{311} residue of PKCδ, accompanied by Tyr^{311} phosphorylated enzyme protein fragments (Fig. 4C), suggesting the association of curcumin with PKCδ directed its degradation which is in agreement with previous work relating PKCδ Tyr^{311} phosphorylation to its increased proteolysis [34].

3.4. *Curcumin enhances NCAM polysialylation state and spatial learning in adult Wistar rats*

Given the transient increase in polysialylated neurons in the hippocampal formation that accompanies consolidation of an avoidance conditioning paradigm [11] is associated with a decrease in PKCδ degradation [27], we determined if curcumin, administered *in vivo*, would similarly increase NCAM polysialylation state in the infragranular zone of the dentate gyrus of adult rats (postnatal day 80). Following daily administration of curcumin (75 mg/kg by gavage) for an 8-day period, we counted a two-fold increase in polysialylated dentate neurons ($P < 0.05$, Student's two-tailed *t*-test) (Fig. 5B). Moreover, the arborisation of these polysialylated neurons in the upper granule cell layers and inner molecular layer was substantially increased, suggesting curcumin induced a remodelling of the dentate neuronal architecture (Fig. 5A).

Curcumin-induced change in dentate NCAM polysialylation state also correlated with improved acquisition and consolidation of the water maze spatial learning paradigm in cohorts of both adult (postnatal day 80) and aged (postnatal day 540) Wistar rats. Adult animals treated with curcumin exhibited a significant difference in task acquisition over four sessions ($F[1,72] = 4.34$, $P = 0.041$; two-way repeated measure ANOVA), as compared to the vehicle-treated controls (Fig. 6A). These animals also spent significantly more time in the target quadrant during subsequent probe trials ($F[1,72] = 3.9$, $P = 0.05$; two-way repeated measure ANOVA) and this became significant at the 72 h recall time (Fig. 6B), as judged by Bonferroni

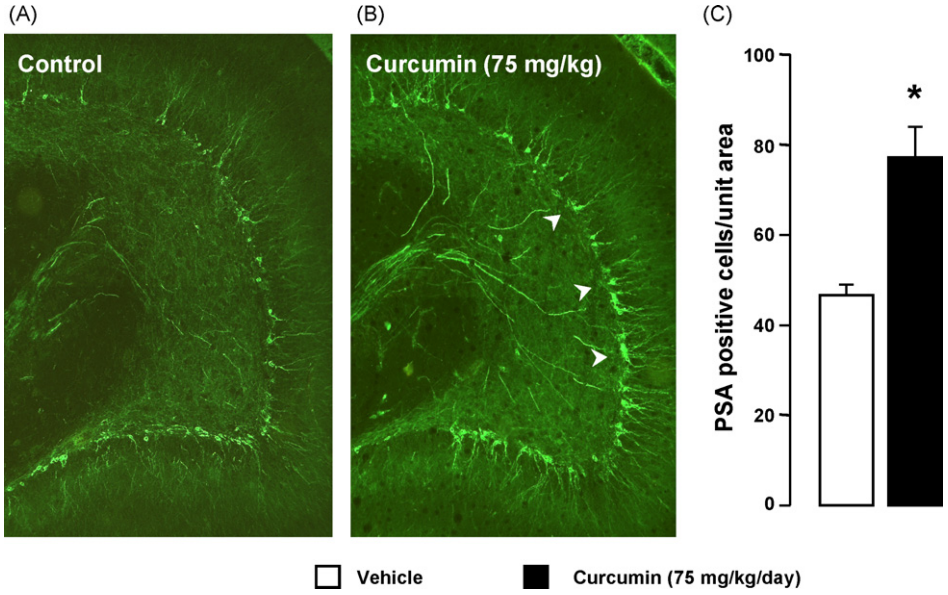

Fig. 5 – Influence of chronic curcumin administration on polysialylated cell frequency in the infragranular zone of the hippocampal dentate gyrus of the adult Wistar rat (postnatal day 80). (A and B) A qualitative comparison of dentate polysialylated cells (see arrow heads in B) and (C) represents their quantitative analysis. The animals received 75 mg/kg curcumin by gavage each day for 8 days. All data are expressed as the mean ± SEM ($n = 3$) and values significantly different ($P < 0.05$) from the vehicle-treated controls are indicated with an asterisk.

post-test and Mann–Whitney *U*-test ($P < 0.05$). These results demonstrated curcumin treatment to exert a marked improvement on both the acquisition and consolidation of the spatial learning task. Curcumin treatment also resulted in significant improvements in both acquisition and consolidation of the water maze task in the cohort of aged animals. Drug-treated animals exhibited a superior performance to their vehicle-treated controls in task acquisition when assessed over four training sessions ($F[1,40] = 6.7$, $P = 0.01$; two-way repeated measure ANOVA) (Fig. 6C). Moreover, curcumin treatment produced a most significant effect on task recall when measured at both the 24 and 72 h probe trials (Fig. 6D), as judged by a two-way repeated measure ANOVA ($F[1,44] = 8.2$, $P = 0.006$) and Bonferroni post-test and Mann–Whitney *U*-test ($P < 0.05$).

4. Discussion

These studies have demonstrated increased PKCδ degradation by curcumin to be associated with an enhanced expression of NCAM polysialylation state in mouse neuro-2A neuroblastoma cells. The ability of curcumin to suppress PKCδ expression is consistent with our previous *in vitro* observations demonstrating phorbol activation and/or staurosporine inhibition of PKCδ to, respectively, suppress and/or enhance PST activity with the direct consequence of regulating the extent to which NCAM is glycosylated with extended chains of PSA [21]. The mechanism by which curcumin induces degradation of PKCδ appears to be associated with increased phosphorylation of the Tyr^{311}residue, which lies within the hinge region between the regulatory and catalytic domains of the enzyme. This finding agrees with previous studies, which have demonstrated phosphorylation of the Tyr^{311} residue to first activate PKCδ and subsequently render it more susceptible to degradation [34] when the hinge region becomes accessible to proteolytic cleavage during the conformational changes associated with enzyme activation [33]. Activation of PKCδ by phorbol esters is also known to trigger their ubiquitination and degradation [43]. Moreover, the Tyr^{311} residue of PKCδ is flanked by a sequence that forms an optimal binding substrate for the Src family of kinases that constitutively complex with PKCδ but not other PKC isoforms such as PKCα or PKCε [44].

Chronic administration of curcumin *in vivo* was also demonstrated to enhance the polysialylation of neurons in the infragranular zone of the dentate gyrus and this included their dendritic tree, which extends into the inner third of the molecular layer. α-Tocopherol, which also reduces PKCδ expression [45], has been found to similarly enhance the polysialylation of neurons in the adult dentate gyrus and, moreover, generate greater complexity in their dendritic arbour, as evidenced by increased synaptophysin expression and synapse density in the molecular layer [46]. Upregulation of dentate NCAM PSA may also, in part, provide a basis for the neuroprotective actions attributed to curcumin [47] as chronic exposure to deprenyl, purported to slow nigral cell degeneration in Parkinson's disease [48], has been demonstrated to increase the frequency of dentate polysialylated cells [49]. Moreover, hyperthermia-induced upregulation of NCAM PSA appears to similarly protect against kainate-induced cell death [50]. Curcumin has been demonstrated to significantly increase the number of newly generated cells in the dentate infragranular zone [51], however, not all of these are polysialylated [52]. The ability of curcumin to enhance neuronal polysialylation through suppression of PKCδ activity may more likely relate to the integration of newborn cells into

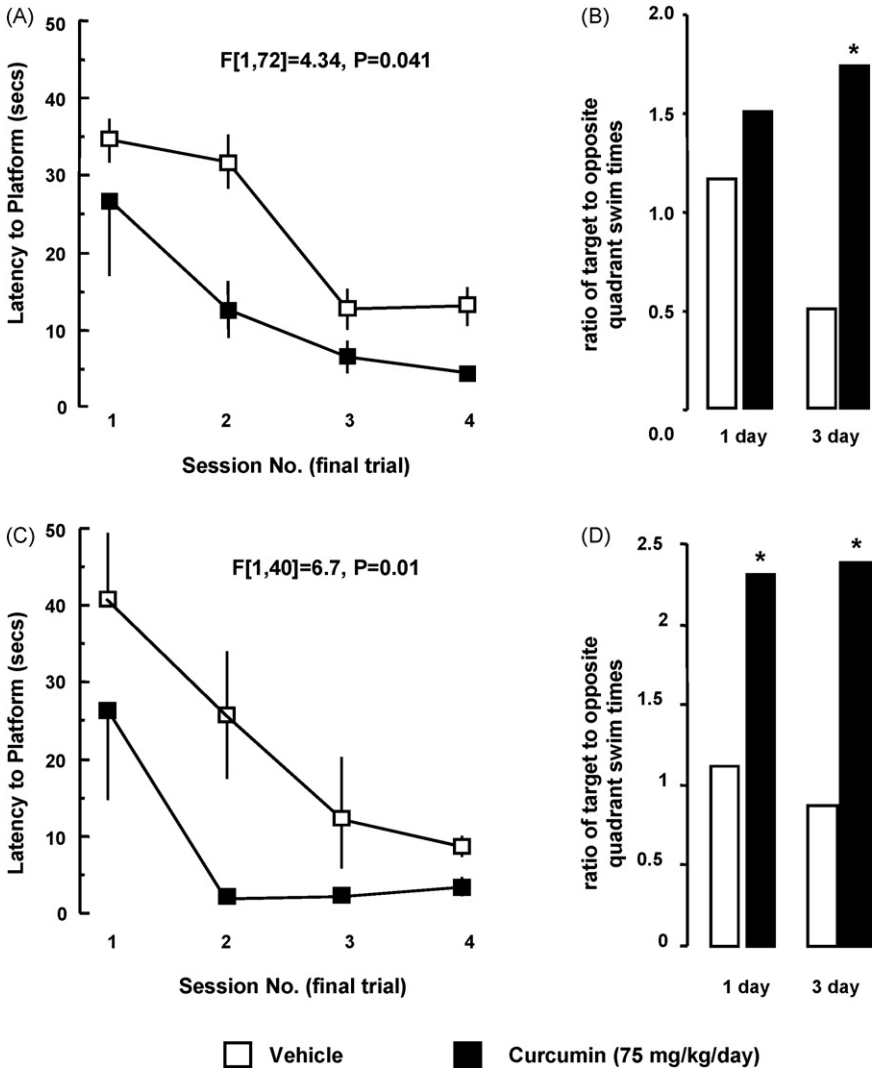

Fig. 6 – Influence of chronic administration of curcumin on spatial learning in adult and aged Wistar rats. (A and B) The influence of curcumin on acquisition and consolidation, respectively, of the water maze paradigm in adult animals. Task acquisition was carried out over four daily sessions of five trials and consolidation was assessed by determining recall at 24 and 72 h following the last training session. (C and D) The same data for the aged animal group. Both the adult (n = 10 for both vehicle and curcumin groups) and aged (n = 7 for vehicle group, n = 5 for the aged group) cohorts received 75 mg/kg curcumin by gavage each day for 8 days. Significant difference in task acquisition over four daily sessions was determined using a two-way repeated measure ANOVA with Bonferroni post-hoc test and Mann–Whitney U-test employed to determine significance at the 24and 72 h recall times (*$P < 0.05$ vs. vehicle).

the dentate neuronal architecture over the 1–2 months period that follows their birth [53–55]. This mechanism would be consistent with the transient decrease in PKCδ expression and associated increase in dentate polysialylated cell frequency that is observed at the 12 h post-training time following avoidance conditioning [11,27] and with other studies that have failed to implicate increased NCAM PSA-mediated plasticity with neurogenesis [11,56,17,50].

Chronic administration of curcumin to adult Wistar rats significantly improved their performance in both the acquisition and consolidation of the water maze spatial learning paradigm. This is not surprising given that chronic administration of curcumin produces a two-fold increase in the frequency of polysialylated dentate neurons, the numerical density of which may be directly correlated to improvement in task performance [57,49]. Environmental enrichment, for example, robustly improves spatial learning and memory and is associated with increased NCAM polysialylation [58,49] and also a decreased expression of PKCδ [27]. Moreover, a pyrazole analogue of curcumin [59] has been demonstrated to facilitate the induction of LTP and performance in an object recognition paradigm in Wistar rats through the induction of Ca^{2+}/calmodulin-dependent protein kinase II [60], a mechanism known to be necessary for both spatial learning and NCAM-mediated neuroplasticity [61,62]. Although, the dose of curcumin required to enhance NCAM polysialylation and cognition *in vivo* was relatively high (75 mg/kg), no effect on either parameter was found at a dose of 37.5 mg/kg (data not

shown), it was within the range previously reported necessary to induce neuroprotective effects *in vivo* [63,64]. Moreover, the dose at which curcumin mediates these neuroplastic actions is likely to be exceptionally low as its bioavailability is exceedingly poor, the majority being excreted in the faeces, and only small fraction of the dose penetrates the brain, estimated to be approximately 0.3% of the administered dose in mice [65,47]. The lack of any behavioural toxicity in these studies, and those of others in both animals and humans [66,67], further implies the effective dose of curcumin necessary to enhance NCAM PSA expression and cognition to be exceptionally small. This unique action of curcumin may have significant implications in facilitating memory formation, as the extent of PSA activation is commensurate with the difficulty experienced with task consolidation [57].

Curcumin also significantly improved spatial learning ability in aged animals despite the significant age-dependent decrease in NCAM polysialylation state [28] and increase in PKCδ expression [27]. However, extensive NCAM polysialylation is not necessary for the acquisition and/or consolidation of behavioural paradigms in aged animals [68,18] and appears to relate mainly to the graded, experience-expectant development of explicit memory systems that continue to evolve into maturity [69]. Curcumin can also regulate the *in vivo* expression of several other cell signalling systems required for neuroplastic events necessary for memory formation, notably Notch-1 and nuclear factor kappa B (NFκB) [70–74]. Nevertheless, facilitation of PSA activation by curcumin, however minimal, may have implications for the treatment of neurodegenerative conditions. In Alzheimer's disease, the natural autoprotective response to age-related cognitive deficits is a small, but significant, activation of dentate polysialylated cell frequency [75] and, over the past few years, an increasing number of studies have highlighted the therapeutic potential of curcumin for the treatment of this condition [76,77], a suggestion further supported by its ability to reduce β-amyloid plaque burden in animal models [78]. Moreover, human populations exposed to curcumin show significantly reduced incidence of Alzheimer's disease, but not apolipoprotein E (ApOE) polymorphisms [79], and improved cognitive ability as compared to a control group [80].

Acknowledgements

We would like to thank Suzanne Prenter for technical assistance. This work was supported by Enterprise Ireland. Marie Lawlor was the recipient of an IRCSET scholarship.

REFERENCES

[1] Sadoul R, Hirn M, Deagostini-Bazin H, Rougon G, Goridis C. Adult and embryonic mouse neural cell adhesion molecules have different binding properties. Nature 1983;30:347–9.
[2] Rougon G, Dubois C, Buckley N, Magnani JL, Zollinger W. A monoclonal antibody against meningococcus group B polysaccharides distinguishes embryonic from adult N-CAM. J Cell Biol 1986;103:429–37.
[3] Bonfanti L. PSA-NCAM in mammalian structural plasticity and neurogenesis. Prog Neurobiol 2006;80:129–64.
[4] Gascon E, Vutskits L, Kiss JZ. Polysialic acid-neural cell adhesion molecule in brain plasticity: from synapses to integration of new neurons. Brain Res Rev 2007;56:101–18.
[5] Rutishauser U. Polysialic acid in the plasticity of the developing and adult vertebrate nervous system. Nat Rev Neurosci 2008;9:26–35.
[6] Hoyk ZS, Parducz A, Theodosis DT. The highly sialylated isoform of the neural cell adhesion molecule is required for estradiol-induced morphological plasticity in the adult arcuate nucleus. Eur J Neurosci 2001;13:649–56.
[7] Stoenica L, Senkov O, Gerardy-Schahn R, Weinhold B, Schachner M, Dityatev A. *In vivo* synaptic plasticity in the dentate gyrus of mice deficient in the neural cell adhesion molecule NCAM or its polysialic acid. Eur J Neurosci 2006;23:2255–64.
[8] O'Malley A, O'Connell C, Regan CM. Ultrastructural analysis reveals avoidance conditioning to induce a transient increase in hippocampal dentate spine density in the 6 h post-training period of consolidation. Neuroscience 1998;87:607–13.
[9] O'Malley A, O'Connell C, Murphy KJ, Regan CM. Transient spine density increases in the mid-molecular layer of the hippocampal dentate gyrus accompany consolidation of a spatial learning task in the rodent. Neuroscience 2000;99:229–32.
[10] Eyre MD, Richter-Levin G, Avital A, Stewart MG. Morphological changes in the hippocampal dentate gyrus synapses following spatial learning in rats are transient. Eur J Neurosci 2003;17:1973–80.
[11] Fox GB, O'Connell AW, Murphy KJ, Regan CM. Memory consolidation induces a transient and time-dependent increase in the frequency of NCAM-polysialylated cells in the adult rat hippocampus. J Neurochem 1995;65:2796–7.
[12] Murphy KJ, O' Connell AW, Regan CM. Repetitive and transient increases in hippocampal neural cell adhesion molecule polysialylation state following multi-trial spatial training. J Neurochem 1996;67:1268–74.
[13] Sandi C, Merino JJ, Cordero MI, Kruyt N, Murphy KJ, Regan CM. Modulation of hippocampal NCAM polysialylation by stressful experiences. Biol Psychiatry 2003;15:599–607.
[14] Becker CG, Artola A, Gerardy-Schahn R, Becker T, Welzl H, Schachner M. The polysialic acid modification of the neural cell adhesion molecule is involved in spatial learning and hippocampal long-term potentiation. J Neurosci Res 1996;45:143–52.
[15] Muller D, Wang C, Skibo G, Toni N, Cremer H, Calaora V, et al. PSA-NCAM is required for activity-induced synaptic plasticity. Neuron 1996;17:413–22.
[16] Venero C, Herrero AI, Touyarot K, Cambon K, López-Fernández MA, Berezin V, et al. Hippocampal up-regulation of NCAM expression and polysialylation plays a key role on spatial memory. Eur J Neurosci 2006;23:1585–95.
[17] López-Fernández MA, Montaron M-F, Varea E, Rougon G, Venero C, Abrous DN, et al. Upregulation of polysialylated neural cell adhesion molecule in dorsal hippocampus after contextual fear conditioning is involved in long-term memory formation. J Neurosci 2007;27:4552–61.
[18] Seymour CM, Foley AG, Murphy KJ, Regan CM. Intraventricular infusions of anti-NCAM PSA impair the process of consolidation of both avoidance conditioning and spatial learning paradigms in Wistar rats. Neuroscience 2008;157:813–20.
[19] Scheidegger EP, Sternberg LR, Roth J, Lowe JB. A human STX cDNA confers polysialic acid expression in mammalian cells. J Biol Chem 1995;270:22685–8.
[20] Yoshida Y, Kojima N, Kurosawa N, Hamamoto T, Tsuji S. Molecular cloning of Sia alpha 2,3Gal beta 1,4GlcNAc alpha

2,8-sialyltransferase from mouse brain. J Biol Chem 1995;270:14628–33.
[21] Eckhardt M, Mühlenhoff M, Bethe A, Koopman J, Frosch M, Gerardy-Schahn R. Molecular characterization of eukaryotic polysialyltransferase-1. Nature 1995;373:715–8.
[22] Nakayama J, Fukuda MN, Fredette B, Ranscht B, Fukuda M. Expression cloning of a human polysialyltransferase that forms the polysialylated neural cell adhesion molecule present in embryonic brain. Proc Natl Acad Sci USA 1995;92:7031–5.
[23] Hildebrandt H, Becker C, Murau M, Gerardy-Schahn R, Rahmann H. Heterogenous expression of the polysialyltransferases ST8Sia II and ST8Sia IV during postnatal rat brain development. J Neurochem 1998;71:2339–48.
[24] Ong E, Nakayama J, Angata K, Reyes L, Katsuyama T, Arai Y, Fukuda M. Developmental regulation of polysialic acid synthesis in mouse directed by two polysialyltransferases, PST and STX. Glycobiology 1998;8:415–24.
[25] Alcaraz G, Goridis G. Biosynthesis and processing of polysialylated NCAM by AtT20 cells. Eur J Cell Biol 1991;55:165–73.
[26] Gallagher HC, Odumeru OA, Regan CM. Regulation of neural cell adhesion molecule polysialylation state by cell–cell contact and protein kinase C delta. J Neurosci Res 2000;61:636–45.
[27] Gallagher HC, Murphy KJ, Foley AG, Regan CM. Protein kinase C delta regulates neural cell adhesion molecule polysialylation state in the rat brain. J Neurochem 2001;77:425–34.
[28] Fox GB, Kennedy N, Regan CM. Polysialylated neural cell adhesion molecule expression by neurons and astroglila processes in the rat dentate gyrus declines dramatically with increasing age. Int J Dev Neurosci 1995;13:663–72.
[29] Gu X, Preuβ U, Gu T, Yu RK. Regulation of sialyltransferase activities by phosphorylation and dephosphorylation. J Neurochem 1995;64:2295–302.
[30] Gao L, Gu X-B, Yu DS, Yu RK, Zeng G. Association of a 14-3-3 protein with CMP-NeuNAc: GM1 α2,3-sialyltransferase. Biochem Biophys Res Commun 1996;224:103–7.
[31] Ma J, Siminovic M, Qian R, Colley KJ. Sialyltransferase isoforms are phosphorylated in the cis-medial Golgi on serine and threonine residues in their luminal sequences. J Biol Chem 1999;274:8046–52.
[32] Breen KC, Georgopoulou N. The role of protein phosphorylation in α2,6(N)-sialyltransferase activity. Biochem Biophys Res Commun 2003;309:32–5.
[33] Kishimoto A, Mikawa K, Hashimoto K, Yasuda I, Tanaka S, Tominaga M, et al. Limited proteolysis of protein kinase C subspecies by calcium-dependent neutral protease (calpain). J Biol Chem 1989;264:4088–92.
[34] Blake RA, Garcia-Paramio P, Parkera PJ, Courtneidge SA. Src promotes PKCδ degradation. Cell Growth Diff 1999;10:231–41.
[35] Gschwendt M, Muller HJ, Kielbassa K, Zang R, Kittstein W, Rincke G, et al. Rottlerin, a novel protein kinase inhibitor. Biochem Biophys Res Commun 1994;199:93–8.
[36] Davies SP, Reddy H, Caivano M, Cohen P. Specificity and mechanism of action of some commonly used protein kinase inhibitors. Biochem J 2000;351:95–105.
[37] Soltoff SP. Rottlerin: an inappropriate and ineffective inhibitor of PKCδ. Trends Pharmacol Sci 2007;28:453–8.
[38] Lipinski CA, Lombardo F, Dominy BW, Feeney FP. Experimental and computational approaches to estimate solubility and permeability in drug discovery and development settings. Adv Drug Deliv Rev 1997;23: 3–25.
[39] Godl K, Wissing J, Kurtenbach A, Habenberger P, Blencke S, Gutbrod H, et al. An efficient proteomics method to identify the cellular targets of protein kinase inhibitors. Proc Natl Acad Sci USA 2003;100:15434–9.
[40] Zhang G, Kazanietz MG, Blumberg PM, Hurley JH. Crystal structure of the cys2 activator-binding domain of protein kinase C delta in complex with phorbol ester. Cell 1995;81:917–24.
[41] Wang YJ, Pan MH, Cheng AL, Lin LI, Ho YS, Hsieh CY, et al. Stability of curcumin in buffer solutions and characterization of its degradation products. J Pharm Biomed Anal 1997;15:1867–76.
[42] Mizuno K, Saido TC, Ohno S, Tamaoki T, Suzuki K. Staurosporine-related compounds, K252a and UCN-01, inhibit both cPKC and nPKC. FEBS Lett 1993;330:114–6.
[43] Lu Z, Liu D, Hornia A, Devonish W, Pagano M, Foster DA. Activation of protein kinase C triggers its ubiquitination and degradation. Mol Cell Biol 1998;18:839–45.
[44] Steinberg SF. Distinctive activation mechanisms and functions for protein kinase Cdelta. Biochem J 2004;384:449–59;
Zingg JM, Azzi A. Non-antioxidant activities of vitamin E. Curr Med Chem 2004;11:1113–33.
[45] Zingg JM, Azzi A. Non-antioxidant activities of vitamin E. Curr Med Chem 2004;11:1113–33.
[46] Ferri P, Cecchini T, Ambrogini P, Betti M, Cuppini R, Del Grande P, et al. α-Tocopherol affects neuronal plasticity in adult rat dentate gyrus: the possible role of PKCδ. J Neurobiol 2006;66:793–810.
[47] Goel A, Kunnumakkara AB, Aggarwal BB. Curcumin as ''Curecumin'': from kitchen to clinic. Biochem Pharmacol 2008;75:787–809.
[48] Ebadi M, Sharma S, Shavali S, El Reaey H. Neuroprotective actions of selegiline. J Neurosci Res 2002;67:285–9.
[49] Murphy KJ, Foley AG, O'Connell AW, Regan CM. Chronic exposure of rats to cognition enhancing drugs produces a neuroplastic response identical to that obtained by complex environment rearing. Neuropsychopharmacology 2006;31:90–100.
[50] Duveau V, Arthaud S, Rougier A, Le Gal le Salle G. Polysialylation of NCAM is upregulated by hyperthermia and participates in heat shock preconditioning-induced neuroprotection. Neurobiol Dis 2007;26:385–95.
[51] Kim SJ, Son TG, Park HR, Park M, Kim MS, Kim HS, et al. Curcumin stimulates proliferation of embryonic neural progenitor cells and neurogenesis in the adult hippocampus. J Biol Chem 2008;283:14497–505.
[52] Foley AG, Hirst WD, Gallagher HG, Barry C, Hagan JJ, Upton N, et al. The selective 5-HT_6 receptor antagonists SB-271046 and SB-399885 potentiate NCAM-PSA immunolabelling of dentate granule cells, but not neurogenesis, in the hippocampal formation of mature Wistar rats. Neuropharmacology 2008;54:1166–74.
[53] Ge S, Yang CH, Hsu KS, Ming GL, Song H. A critical period for enhanced synaptic plasticity in newly generated neurons of the adult brain. Neuron 2007;54:559–66.
[54] Kee N, Teixeira CM, Wang AH, Frankland PW. Preferential incorporation of adult-generated granule cells into spatial memory networks in the dentate gyrus. Nat Neurosci 2007;10:355–62.
[55] Toni N, Laplagne DA, Zhao C, Lombardi G, Ribak CE, Gage FH, et al. Neurons born in the adult dentate gyrus form functional synapses with target cells. Nat Neurosci 2008;11:901–7.
[56] Pham K, McEwen BS, LeDoux JE, Nader K. Fear learning transiently impairs hippocampal cell proliferation. Neuroscience 2005;130:17–24.
[57] Sandi C, Cordero MI, Merino JJ, Kruyt ND, Regan CM, Murphy KJ. Neurobiological correlates of individual differences in spatial learning ability. Learn Mem 2004;11:244–52.

[58] Young D, Lawlor PA, Leone P, Dragunow M, During MJ. Environmental enrichment inhibits spontaneous apoptosis, prevents seizures and is neuroprotective. Nat Med 1999;5:448–53.
[59] Liu Y, Dargusch R, Maher P, Schubert D. A broadly protective derivative of curcumin. J Neurochem 2008;105:1336–45.
[60] Maher P., Akaishi T., Schubert D., Abe K. A pyrazole derivative of curcumin enhances memory. *Neurobiol Aging* (2008) in press.
[61] Silva AJ, Paylor R, Wehner JM, Tonegawa S. Impaired spatial learning in alpha-calcium-calmodulin kinase II mutant mice. Science 1992;257:206–11.
[62] Williams EJ, Mittal B, Walsh FS, Doherty P. A Ca2+/calmodulin kinase inhibitor, KN-62, inhibits neurite outgrowth stimulated by CAMs and FGF. Mol Cell Neurosci 1995;6:69–79.
[63] Jagatha B, Mythri RB, Vali S, Bharath MMS. Curcumin treatment alleviates the effects of glutathione depletion *in vitro* and *in vivo*: therapeutic implications for Parkinson's disease explained via *in silico* studies. Free Radic Biol Med 2008;44:907–17.
[64] Shukla PK, Khanna VK, Ali MM, Khan MY, Srimal RC. Anti-ischemic effect of curcumin in rat brain. Neurochem Res 2008;33:1036–43.
[65] Ryu EK, Choe YS, Lee KH, Choi Y, Kim BT. Curcumin and dihydrozingerone derivatives: synthesis, radiolabelling, and evaluation for beta-amyloid plaque imaging. J Med Chem 2006;49:6111–9.
[66] Shankar TN, Shanta NV, Ramesh HP, Murthy IA, Murthy VS. Toxicity studies on turmeric (*Curcuma longa*): acute toxicity studies in rats, guineapigs and monkeys. Indian J Exp Biol 1980;18:73–5.
[67] Lao CD, Ruffin MT, Normolle D, Heath DD, Murray SI, Bailey JM, et al. Dose escalation of a curcuminoid formulation. BMC Complement Altern Med 2006;6:10.
[68] Abrous DN, Montaron MF, Petry KG, Rougon G, Darnaudery M, Le Moal M, et al. Decrease in highly polysialylated neuronal cell adhesion molecules and in spatial learning during ageing are not correlated. Brain Res 1997;744:285–92.
[69] Stanton ME. Multiple memory systems, development and conditioning. Behav Brain Res 2000;110:25–37.
[70] Romano A, Freudenthal R, Merlo E, Routtenberg A. Evolutionarily-conserved role of the NF-kappaB transcription factor in neural plasticity and memory. Eur J Neurosci 2006;24:1507–16.
[71] Wang Y, Chan SL, Miele L, Yao PJ, Mackes J, Ingram DK, et al. Involvement of Notch signalling in hippocampal plasticity. Proc Natl Acad Sci USA 2004;101:9458–62.
[72] Chen Y, Shu W, Chen W, Wu Q, Liu H, Cui G. Curcumin, both histone deacetylase and p300/CBP-specific inhibitor, represses the activity of nuclear factor kappa B and Notch 1 in Raji cells. Basic Clin Pharmacol Toxicol 2007;101:427–33.
[73] Conboy L, Seymour CM, Monopoli MP, O'Sullivan NC, Murphy KJ, Regan CM. Notch signalling becomes transiently attenuated during long-term memory consolidation in adult Wistar rats. Neurobiol Learn Mem 2007;88:342–51.
[74] Shishodia S, Singh T, Chaturvedi MM. Modulation of transcription factors by curcumin. Adv Exp Med Biol 2007;595:127–48.
[75] Mikkonen M, Soininen H, Tapiola T, Alafuzoff I, Miettinen R. Hippocampal plasticity in Alzheimer's disease: changes in highly polysialylated NCAM immunoreactivity in the hippocampal formation. Eur J Neurosci 1999;11:1754–64.
[76] Wu A, Ying Z, Gomez-Pinilla F. Dietary curcumin counteracts the outcome of traumatic brain injury on oxidative stress, synaptic plasticity, and cognition. Exp Neurol 2006;197:309–17.
[77] Xu Y, Ku B, Tie L, Yao H, Jiang W, Ma X, et al. Curcumin reverses the effects of chronic stress on behaviour, the HPA axis, BDNF expression and phosphorylation of CREB. Brain Res 2006;1122:56–64.
[78] Begum AN, Jones MR, Lim GP, Morihara T, Kim P, Heath DD, et al. Curcumin structure-function, bioavailability, and efficacy in models of neuroinflammation and Alzheimer's disease. J Pharmacol Exp Ther 2008;326:196–208.
[79] Ganguli M, Chandra V, Kamboh MI, Johnston JM, Dodge HH, Thelma BH, et al. Apolipoprotein E polymorphism and Alzheimer disease. Arch Neurol 2000;57:824–30.
[80] Ng TP, Chiam PC, Lee T, Chua HC, Lim L, Kua EH. Curry consumption and cognitive function in the elderly. Am J Epidemiol 2006;164:898–906.